Article

J. Biol. Regul. Homeost. Agents. 2024; 38(7): 5605–5617
https://doi.org/10.23812/j.biol.regul.homeost.agents.20243807.451

IL-25 Promotes Tumor Progression by Activating the AKT/mTOR Signaling Pathway in Bladder Cancer

Jianglin Shi[1], Zewei Zhao[1], Zhonghan Yang[1,*], Yong Huang[2,3,*]

[1]Shenzhen Key Laboratory of Systems Medicine for Inflammatory Diseases, School of Medicine, Shenzhen Campus of Sun Yat-sen University, 518107 Shenzhen, Guangdong, China
[2]Department of Urology, The First Affiliated Hospital, Sun Yat-sen University, 510080 Guangzhou, Guangdong, China
[3]Department of Emergency, The First Affiliated Hospital, Sun Yat-sen University, 510080 Guangzhou, Guangdong, China
*Correspondence: yangzhh@mail.sysu.edu.cn (Zhonghan Yang); huangy79@mail.sysu.edu.cn (Yong Huang)
Submitted: 14 March 2024 Revised: 15 April 2024 Accepted: 6 May 2024 Published: 1 July 2024

Background: Bladder cancer is a common tumor of the urinary system. Interleukin-25 is highly expressed in a variety of tumors and leads to poor prognosis. However, the expression and biological role of interleukin-25 in bladder cancer remain unclear.
Methods: This study analyzed the differential expression of interleukin-25 (IL-25) and its receptor, interleukin-17 receptor B (IL-17RB), in tumor and adjacent tissues from bladder cancer patients by bioinformatics databases and immunohistochemistry. The impact of IL-25 on bladder cancer cell proliferation and migration was assessed *in vitro*. Moreover, we used wild-type and IL-25 knockout mice implanted with bladder cancer cells to investigate tumor growth *in vivo*. Gene set enrichment analysis (GSEA) was employed to elucidate the underlying mechanisms. We further explored the function of interleukin-25 in bladder cancer by cell viability assay and western blot. Angiogenesis was also compared between the wild-type and IL-25 knockout mice.
Results: Immunohistochemistry indicated a significantly higher expression of IL-25 in bladder cancer tissues, which correlated with several prognostic markers. Analysis of The Cancer Genome Atlas (TCGA) database revealed that IL-17RB was highly expressed in bladder cancer, and may be related to overall survival of patients. *In vitro*, IL-25 enhanced the proliferation and migration of bladder cancer cells. IL-25 knockout markedly reduced tumor growth in a murine subcutaneous bladder cancer model. Mechanistic investigations revealed that IL-25 enhanced bladder cancer cell proliferation by activating the AKT (protein kinase B), mammalian target of rapamycin (mTOR) signaling pathway (AKT/mTOR signaling pathway). Additionally, angiogenesis was suppressed in IL-25 knockout mice bearing bladder tumors.
Conclusion: Our findings suggest that IL-25 promotes bladder cancer cell proliferation by activating the AKT/mTOR signaling pathway and IL-25 knockout inhibits angiogenesis in bladder cancer. These findings suggest that IL-25 is a potential prognostic marker and therapeutic target in bladder cancer management.

Keywords: bladder cancer; interleukin-25; tumor proliferation and migration; blood vessel formation; AKT/mTOR signaling pathway

Introduction

Bladder cancer (BCa) ranks as the fourth most prevalent cancer among men globally and accounts for approximately 90% of all urothelial cancers [1,2]. Based on the degree of invasion, BCa is classified into two main types: muscle-invasive bladder cancer (MIBC) and non-muscle-invasive bladder cancer (NMIBC). Approximately 70% of patients are diagnosed with NMIBC, while 25%–30% present with either muscle-invasion or metastasis at the time of initial diagnosis [3,4]. NMIBC is notably heterogeneous and associated with a high risk of recurrence, with a 5-year recurrence rate of 31%–78% and about 10%–20% of cases progressing to MIBC [5,6]. Given that metastasis and recurrence are significant contributors to mortality in BCa patients [7], understanding the underlying mechanisms that drive BCa progression is crucial for identifying novel therapeutic targets and enhancing patient outcomes.

Interleukin-25 (IL-25), also known as interleukin-17E, is a member of the IL-17 cytokine family, closely related to inflammatory processes [8]. IL-25 is recognized as a type 2 immune mediator, stimulating Th2 cells to release cytokines such as IL-4, IL-5, and IL-13, exacerbating allergic inflammation upon interacting with its receptor, IL-17RB [9]. The role of IL-25 extends beyond modulating inflammatory responses. It has been implicated in suppressing Th1 and Th17 cell differentiation, thus exhibiting anti-inflammatory effects in conditions such as inflammatory bowel disease, type 1 diabetes, and rheumatoid arthritis [10–13]. Furthermore, IL-25 promotes cell proliferation [14,15] and inhibits apoptosis in non-immune cells [16]. Additionally, IL-25 contributes to tissue repair and regeneration as a barrier cytokine [17,18].

In oncology, IL-25 is notably overexpressed in various malignancies, including cholangiocarcinoma [19], hepatoblastoma [20], and mucosal melanoma [21], where it

Journal of
BIOLOGICAL REGULATORS
and Homeostatic Agents

is associated with metastasis and adverse prognosis [19]. Previous investigations have revealed that IL-25 expression is significantly upregulated in liver cancer, contributing to disease progression and metastasis by inducing M2 macrophage polarization and facilitating secretion of the chemokine (C-X-C motif) ligand 10 (CXCL10) [22]. Additionally, IL-25 activates the Hedgehog signaling pathway and promotes glioma-associated oncogene homologue 1 (GLI1) accumulation by inhibiting AMP-activated protein kinase (AMPK) phosphorylation, thereby maintaining tumor stemness in colon cancer [23]. In contrast, Benatar *et al*. [24] have reported an antitumor role of IL-25, which involves inducing Th2 cells to produce IL-5, leading to eosinophilic infiltration and potentially inhibiting tumor growth.

Despite these findings, literature on the association between IL-25 and bladder cancer remains limited. Only one study has investigated this relationship, revealing a decrease in IL-25 and IL-17RB expression alongside reduced neutrophil infiltration in bladder cancer tissues compared to cystitis tissues, as determined through immunohistochemical analysis [25].

These diverse roles underscore the complex contribution of IL-25 in cancer pathogenesis and progression. Bladder cancer is a common urinary tract tumor and its pathogenesis and development mechanisms still need to be further explored. This study aimed to elucidate the pivotal role of IL-25 in the pathogenesis and progression of bladder cancer. This investigation intended to clarify the underlying mechanisms by which IL-25 influences bladder cancer, thereby establishing a scientific foundation for targeting IL-25 as a novel therapeutic approach for bladder cancer.

Materials and Methods

Datasets from TCGA and Bioinformatics Analysis

Gene expression profiles and corresponding clinical information for BCa were retrieved from the The Cancer Genome Atlas (TCGA) database (https://portal.gdc.cancer.gov/) using the R package "TCGAbiolinks". The dataset comprised 415 BCa and 19 adjacent tissues samples, with RNA-seq (fragments per kilobase of transcript per million fragments mapped, FPKM) data available for 19,752 genes. Following data retrieval, probe-to-gene symbol conversion was performed according to the annotation file, and all expression profiles were normalized by transforming them into $\log_2$(FPKM+1) for subsequent analysis.

For the expression analysis of IL-17RB, all downloaded data, consisting of 414 tumor samples and 19 adjacent tumor samples, were utilized. For IL-25 expression analysis, 151 tumor samples and 7 paracancer samples were selected for analysis after removing null values and identifying one outlier. Survival analysis was conducted using the online analysis tool gene expression profiling interactive analysis 2 (GEPIA2) (http://gepia2.cancer-pku.cn/#survival). The group cutoff is set as the quartile, and the high expression group accounts for 25% and the low expression group accounts for 75%.

Human Bladder Cancer Clinical Sample Collection

A total of 49 bladder cancer tumor specimens and corresponding para-cancer tissue samples were procured between May 2017 and September 2018 from the First Affiliated Hospital of Sun Yat-sen University. Following resection, the tissue specimens were divided: one part was fixed by immersion in 4% paraformaldehyde (G1101, Servicebio, Wuhan, China), while the other part was immediately stored at –80 °C for long-term preservation. All patients provided informed consent, and the study protocol was approved by the Ethics Committee of the First Affiliated Hospital of Sun Yat-sen University (IRB no. [2019] 342).

Inclusion criteria comprised patients with confirmed pathological diagnosis of bladder malignancy without any preoperative chemotherapy, radiotherapy, or other tumor-related interventions. Clinicopathological data, including gender, age, pathological grade, and TNM (T, Topography; N, Lymph Node; M, Metastasis) stage, were recorded for each patient. Regular follow-up assessments were conducted to monitor recurrence, distant metastasis, and overall survival. Detailed patient information is presented in **Supplementary Table 1**.

Immunohistochemistry Assay

All tissue specimens were fixed in 4% paraformaldehyde and subsequently paraffin-sectioned by Wuhan Service-bio Co., Ltd. Immunohistochemical staining of the sections was performed following the outlined protocol. Briefly, sections were deparaffinized in an oven for 30 minutes and then hydrated in gradient ethanol. After completion, the sections were immersed in 0.01 M citrate buffer (pH 6.0, X861541-10EA, macklin, Shanghai, China) for antigen retrieval by the high-pressure method. The sections were then immersed in 3% H_2O_2 (H_2O_2-500 mL, LIRCON, Guangzhou, China) to quench endogenous peroxidase. The sections were placed in cassette, circled along the edge of the sample with an immunohistochemical (IHC) pen, and blocked with goat serum drops for 1 hour. After removing the blocking solution, primary antibodies were applied and incubated overnight at 4 °C: IL-25 (1:200; NB100-56541, Novus Biologicals, Littleton, CO, USA) and CD31(1:200; GB11063-2, Servicebio, Wuhan, China).

The following day, primary antibodies were removed, and HRP-labeled secondary antibody (1:200, G1213/G1214, Servicebio, Wuhan, China) was applied and incubated for 1 hour at room temperature. Subsequently, cells were stained using a DAB kit (G1212-200T, Servicebio, Wuhan, China) and counterstained with hematoxylin. Following completion of staining, slides were sealed with neutral resin, and sections were allowed to dry overnight. Finally, images were captured using a slide scanner (Axio

Scan. Z1, ZEISS, Oberkochen, BW, Germany) or Olympus BX63 (Olympus, Tokyo, Japan). The degree of IHC staining was assessed in a single-blind manner by a physician and determined by the staining index (SI). SI was calculated as the product of the tumor cell proportion grade and staining intensity score [26]. Microvessel density was quantified through CD31 immunohistochemical staining.

Cell Culture

Human bladder cancer cell lines T24, BIU87, and 5637 were generously provided by Guoquan Gao's Laboratory, Sun Yat-sen University School of Medicine. MB49 cells were derived from bladder transitional cell carcinoma induced by carcinogens in C57BL/6 male mice and were procured from Guangzhou Suyan Biotechnology Co., Ltd., Guangzhou, China. Cells were authenticated by STR analysis and routinely confirmed free of mycoplasma contamination. T24, BIU87, and 5637 cells were cultured in RPMI1640 medium (GIBCO) supplemented with 10% inactivated Fetal Bovine Serum (FBS, 10099141C, GIBCO, Qunxian Technology, Guangzhou, China) and 1% penicillin-streptomycin (15140-122, GIBCO, Meilun Biotechnology, Guangzhou, China). Cells were maintained in an incubator at 37 °C with 5% CO_2.

MB49 cells were cultured in Dulbecco's modification of Eagle's medium (DMEM, C11995500BT, GIBCO, Jiayan Biotechnology, Guangzhou, China) containing 4.5 g/L glucose, supplemented with 10% inactivated FBS and 1% penicillin-streptomycin. Similar incubator conditions were set for MB49 cells. Following a 12-hour starvation period, cell culture medium was supplemented with recombinant human IL-25 (10096-H01H, Sinobiological, Beijing, China) or recombinant mouse IL-25 (50138-M07H, Sinobiological, Beijing, China) in a dose-dependent manner. Additionally, siRNA molecules (Generay, Shanghai, China) were transfected into MB49 cells to knockdown IL-25 using Lipofectamine™3000 transfection reagent (L3000015, ThermoFisher, Waltham, MA, USA). The sequences of siRNA are provided in **Supplementary Table 2**.

Enzyme-Linked Immunosorbent Assays (ELISA)

The IL-25 levels in cell culture supernatants were quantified using the Human IL-17E ELISA Kit (EHC180.96, Neobioscience, Haobo Biotechnology, Guangzhou, China). Three human bladder cancer cell lines, T24, BIU87 and 5637, were seeded in 12-well cell culture plates at a density of approximately 5×10^5 cells per well with triplicate wells. Cells were cultured in a serum-free medium at 37 °C with 5% CO_2 for 24 hours.

Subsequently, 300 µL of cell culture supernatant was collected from each well for ELISA analysis. All procedures were performed following the manufacturer's standard protocol for the kit.

Colony Formation Assay

After digestion into a single-cell suspension, bladder cancer cells were seeded at densities of 500 or 1000 cells per well in a 6-well cell culture plate. After a 12-hour starvation period, the cell culture medium was supplemented with recombinant human IL-25 (10096-H01H, Sinobiological, Beijing, China) or recombinant mouse IL-25 (50138-M07H, Sinobiological, Beijing, China) in a dose-dependent manner. Additionally, siRNA molecules (Generay, Shanghai, China) were transfected into MB49 cells to knockdown IL-25 using Lipofectamine™3000 transfection reagent (L3000015, ThermoFisher, Waltham, MA, USA) before digestion and seeding. Cells were cultured in a complete culture medium for approximately 1 week at 37 °C with 5% CO_2, and the culture was terminated upon the formation of more than 50 monoclonal colonies. Subsequently, cells were fixed with 4% paraformaldehyde for 10 minutes and stained with 0.1% crystal violet solution (G1014-50ML, Servicebio, Wuhan, China). Finally, the culture plates were scanned using an image scanner, and the number of cell colonies formed was quantified using Image J 1.8.0 (National Institutes of Health, Bethesda, MD, USA).

Cell Viability Assay

Cell viability was assessed using the Cell Counting Kit-8 (CCK-8, CK04, Dojindo, Zuoke Biotechnology, Guangzhou, China). The experimental protocols were as follows: Bladder cancer cells were seeded in 96-well plates at densities ranging from 3000 to 5000 cells per well. After a 12-hour starvation period, MB49 cells were treated with either 50 ng/mL of IL-25 or 0.5 µM of mTOR inhibitor AZD8055 (SC0042-10 mM, Beyotime, Shanghai, China) for 48 hours. Subsequently, 10 µL of CCK-8 solution was added to each well, and after incubation for 2 hours, the absorbance at 450 nm was measured as the OD value using a Sunrise microplate reader (Sunrise, TECAN, Maannedorf, Switzerland).

Transwell Migration Assay

A Transwell chamber with a 24-well plate format (CN-3422, Corning, Kerong Biology, Guangzhou, China) featuring an 8.0 µm pore size membrane was used for the migration assay. Firstly, 600 µL DMEM medium supplemented with 20% FBS was added to the lower chamber. Subsequently, bladder cancer cells were detached into single-cell suspension using trypsin, approximately 1×10^5 cells in 100 µL of serum-free medium were seeded into each well of the upper chamber. Following a 24-hour incubation period, cells on the outer side of the chamber membrane were gently removed with a cotton swab. The migrated cells on the inner side of the membrane were fixed with 4% paraformaldehyde for 10 minutes and stained with 0.1% crystal violet solution. Finally, the transwell chambers were observed and imaged under an inverted fluorescence microscope (Leica DMI4000B, Wetzlar, Germany).

Journal of
BIOLOGICAL REGULATORS
and Homeostatic Agents

Experimental Animals

Female wild-type C57/BL6 mice (6 weeks old, weighing 16–18 g) were procured from Guangdong Medical Laboratory Animal Center, with Animal Production license number SCXK (Guangdong) 2018-0002. IL-25 knockout (IL-25KO) mice with a C57BL/6J genetic background were obtained from the Model Animal Research Center of Nanjing University. All mice were housed at the Laboratory Animal Center of Sun Yat-sen Medical College, and the experimental procedures were approved by the Institutional Animal Care and Use Committee (IACUC) of Sun Yat-sen University (Approval No. SYSU-IACUC-MED-2023-B082).

Construction of Subcutaneous Transplantation Tumor Model of Bladder Cancer

For bladder cancer transplanted tumor model, 2×10^6 MB49 cells were suspended in 100 µL of serum-free DMEM medium and injected subcutaneously under the right axilla of the mice. After a week, the tumor volume was monitored by measuring the length (a) and width (b) of the tumor with a vernier caliper and calculated using the formula $V = (a^2 \times b)/2$, where "b" represents the longest axis and "a" is the perpendicular axis to b.

On day 25 post-injection, mice were euthanized via cervical dislocation. Tumor tissues and adjacent normal bladder tissues were collected. Tumor tissues were photographed and weighed, and a portion was fixed in 4% paraformaldehyde for paraffin sectioning, while the remainder was stored at –80 °C for further analysis.

Real-Time PCR Analysis

RNA extraction from tissues or cells was conducted using TRIZOL reagent (#15596026, Invitrogen, Carlsbad, CA, USA), and RNA concentration was determined using a nanodrop 2000. Reverse transcription was performed using SweScript All-in-One-First-Strand cDNA Synthesis SuperMix (G3337-100, Servicebio, Wuhan, China). Subsequently, the system was prepared with SYBR Green qPCR Master Mix (G3326-15, Servicebio, Wuhan, China), and real-time PCR analysis was performed using either the CFX96 (BioRad, Hercules, CA, USA) or the LightCycler480II (Roche, Basel, Switzerland). The PCR primer sequences used for PCR amplification are listed in **Supplementary Table 3**.

Western Blotting

Cells were lysed by adding SDS buffer to the plates, supplemented with 1 mM phenylmethane sulfonyl fluoride (ST506, Beyotime, Shanghai, China), 1× phosphatase inhibitor (HY-K0021, MCE, Shanghai China), and 1× protease inhibitor cocktail (HY-K0010, MCE, Shanghai, China) to prevent protein degradation. The entire procedure was performed on ice. Total protein (30 µg) was loaded onto a polyacrylamide gel for western blotting after protein concentration was determined using a BCA kit (KGP902, KeyGen, Nanjing, China). Proteins were transferred onto 0.45 mm or 0.22 mm PVDF membranes (IPVH00010-N1 and ISEQ00010-N1, Millipore, Tangsui Technology, Guangzhou, China) via electrotransfer, followed by blocking with 7% nonfat milk in TBST (G2150, Servicebio, Wuhan, China) for 1 hour.

The membranes were then incubated with the following primary antibodies: IL-25 (1:1000; SRP05297, Saierbio, Tianjin, China); pan-AKT1/2/3 Ab (1:1000; AF6261, Affbiotech, Guangzhou, China), Phospho-pan-AKT1/2/3 (Ser473) (1:1000; AF0016, Affbiotech, Guangzhou, China); ribosomaiprotein S6 kinase 1 (S6K1, 1:1000; GB111133, Servicebio, Wuhan, China), CD31 (1:1000; GB11063-2, Servicebio, Wuhan, China), heat shock protein 90 (HSP90, 1:2000; GB12284, Servicebio, Wuhan, China); Cyclin D1 (1:1000; WL01435a, Wanleibio, Shenyang, China), proliferating cell nuclear antigen (PCNA, 1:1000; WL03213, Wanleibio, Shenyang, China); Phospho-P70 S6K (Thr389, 1:1000; AF5899, Beyotime, Shanghai, China). Following overnight incubation at 4 °C, membranes were probed with HRP-conjugated anti-rabbit IgG (1:2000, G1213, Servicebio, Wuhan, China) or anti-mouse IgG (1:2000, G1214, Servicebio, Wuhan, China), then developed using ECL substrate (Merck Millipore, Billerica, MA, USA) and visualized using the Tanon 4600 SF (Tanon, Shanghai, China).

Statistical Analysis

All data were presented as mean ± standard deviation (SD) or mean ± SEM (standard error of mean). GraphPad Prism8.0 (GraphPad, La Jolla, CA, USA) was used to plot graphs and statistical analyses. *T*-test was used to compare data between two groups, while analysis of variance (ANOVA) and Dunnett's test were used to compare more than two groups. For all presented data, significance was denoted as ns (no significance), $*p < 0.05$, $**p < 0.01$, $***p < 0.001$, where $p < 0.05$ was considered statistically significant.

Results

Elevated IL-25 and IL-17RB Were Associated with Tumor Progression in BCa

To explore the pivotal role of IL-25 and its receptor IL-17RB in BCa, we analyzed transcriptome expression profiles from the TCGA database. Our analysis revealed a significant upregulation of IL-17RB expression in BCa tumor tissues compared to adjacent tissues (Fig. 1A). Moreover, survival analysis demonstrated that BCa patients exhibiting high IL-17RB expression had improved overall survival (OS) in the early stages but worse disease-free survival (DFS) in the advanced stages (Fig. 1B), suggesting a dynamic role of IL-17RB in BCa progression.

Transcriptome analysis did not reveal a significant difference in IL-25 expression between BCa tissues and adjacent counterparts (Fig. 1A). However, immunohistochemical analysis of clinical samples illustrated a notably elevated protein expression level of IL-25 in BCa tissues compared to adjacent tissues (Fig. 1C). Combined with the pathological information, we found that the expression of IL-25 in patients with muscle invasion and metastasis was respectively higher than non-muscle invasion and non-metastasis, with stage III patients exhibiting higher expression levels than stage I (Fig. 1D). Although patients with high IL-25 expression exhibited lower survival rates, the difference was not statistically significant ($p = 0.09$, Fig. 1D). In summary, these findings suggest that elevated expressions of IL-25 and its receptor IL-17RB are associated with accelerated progression of BCa.

IL-25 Promotes the Proliferation and Migration of BCa in Vitro and in Vivo

To further investigate the role of IL-25 in BCa progression, we performed *in vitro* cell experiments and *in vivo* BCa transplantation tumor experiments in mice. Our analysis revealed significantly higher IL-17RB expression in BCa cell line BIU87 compared to T24 and 5637 (Fig. 2A). However, no differences were observed in the expression and secretion of IL-25 among these cell lines (Fig. 2A,B). Recombinant human IL-25 was used to treat BIU87 in a concentration-dependent manner, and the results showed that IL-25 promoted its proliferation and migration (Fig. 2C,D). Similar results were observed in mouse bladder cancer MB49 cells (Fig. 2E,G). Additionally, the proliferation of MB49 cells with IL-25 knockdown by siRNA was inhibited (Fig. 2F).

To assess the impact of IL-25 on BCa, we established BCa transplant models in IL-25 knockout (IL-25KO) mice and wild-type (WT) mice through subcutaneous injection of MB49 cells. Notably, tumors in IL-25KO mice exhibited reduced size and weight compared to WT (Fig. 2H,I). These findings suggest that IL-25 promotes the proliferation and migration of bladder cancer.

Potential Influence of IL-25 and IL-17RB on Nucleotide-Binding Oligomerization Domain (NOD)-Like Receptor Signaling Pathways in BCa

A preliminary bioinformatic analysis was performed to further investigate the potential mechanism through which IL-25 influences BCa progression. BCa transcriptome data from the TCGA database were uploaded to the Sangerbox website and categorized using the quartile method into high (75%) and low (25%) IL-17RB expression groups. The gene set enrichment analysis (GSEA) enrichment analysis revealed that the low IL-17RB expression group significantly impacted the NOD-like receptor signaling pathway (NOD: nucleotide-binding oligomerization domain) (**Supplementary Fig. 1A**). Patients in this group exhibited upregulated expression of core genes associated with this signaling pathway (**Supplementary Fig. 1B**). Further experimental investigations were conducted on tumor tissues from mice and a cell line. The results indicated the downregulation of genes in the NOD-like receptor signaling pathway in IL-25KO mice, although these changes were not statistically significant (**Supplementary Fig. 1C**). Nucleotide-binding oligomerization domain protein 2 (*NOD2*), a key component of NOD-like receptors, was significantly reduced in the IL-25KO group compared to the WT group (**Supplementary Fig. 1C**). Conversely, the expression level of *NOD2* in MB49 cells treated with 50 ng/mL IL-25 was significantly higher than untreated group (**Supplementary Fig. 1D**). Similarly, there was no significant difference of other genes compared with the untreated group (**Supplementary Fig. 1D**). These experimental findings suggest that IL-25 exerts a minor modulatory effect on the NOD-like signaling pathway. These bioinformatics results indicate a negative correlation between IL-17RB expression and the expression of core genes in this pathway. Given the variability in the effects of IL-25 and its receptor IL-17RB and the lack of consistent significant impact on NOD-like receptor signaling pathway, further exploration into this mechanism has been suspended.

IL-25 Promotes BCa Cell Proliferation by Activating the AKT/mTOR Signaling Pathway

Previous studies have underscored the pivotal role of the AKT (protein kinase B), mammalian target of rapamycin (mTOR) signaling pathway (AKT/mTOR) signaling pathway in tumor development. To explore whether IL-25 promotes BCa progression by activating the AKT/mTOR signaling pathway, we examined the relative viability of MB49 cells treated with IL-25 and AZD8055, an ATP-competitive mTOR inhibitor. Results from the CCK-8 assay revealed that MB49 cells treated with IL-25 exhibited a significantly higher relative survival rate compared to untreated cells. Interestingly, no significant difference was observed between the AZD8055 treatment group and the IL-25 and AZD8055 co-treatment group (Fig. 3A). These findings suggest that the facilitative effect of IL-25 on proliferation diminishes upon inhibition of the AKT/mTOR signaling pathway (Fig. 3A). Furthermore, the knockdown of IL-25 using siRNA inhibited the proliferation of MB49 cells, as shown in Fig. 3B. Western blot analysis revealed that IL-25 treatment enhanced the phosphorylation levels of AKT and S6K (activated by mTORC1), and the expression level of cell proliferation-related protein was up-regulated, including proliferating nuclear antigen (PCNA) and Cyclin D1 (Fig. 3C). The AKT/mTOR signaling pathway was significantly inhibited and the expressions of PCNA and Cyclin D1 were decreased upon the addition of the mTOR inhibitor (Fig. 3C). Additionally, Fig. 3D exhibits decreased AKT and S6K phosphorylation in MB49 cells following IL-25 knockdown, ac-

Journal of
BIOLOGICAL REGULATORS
and Homeostatic Agents

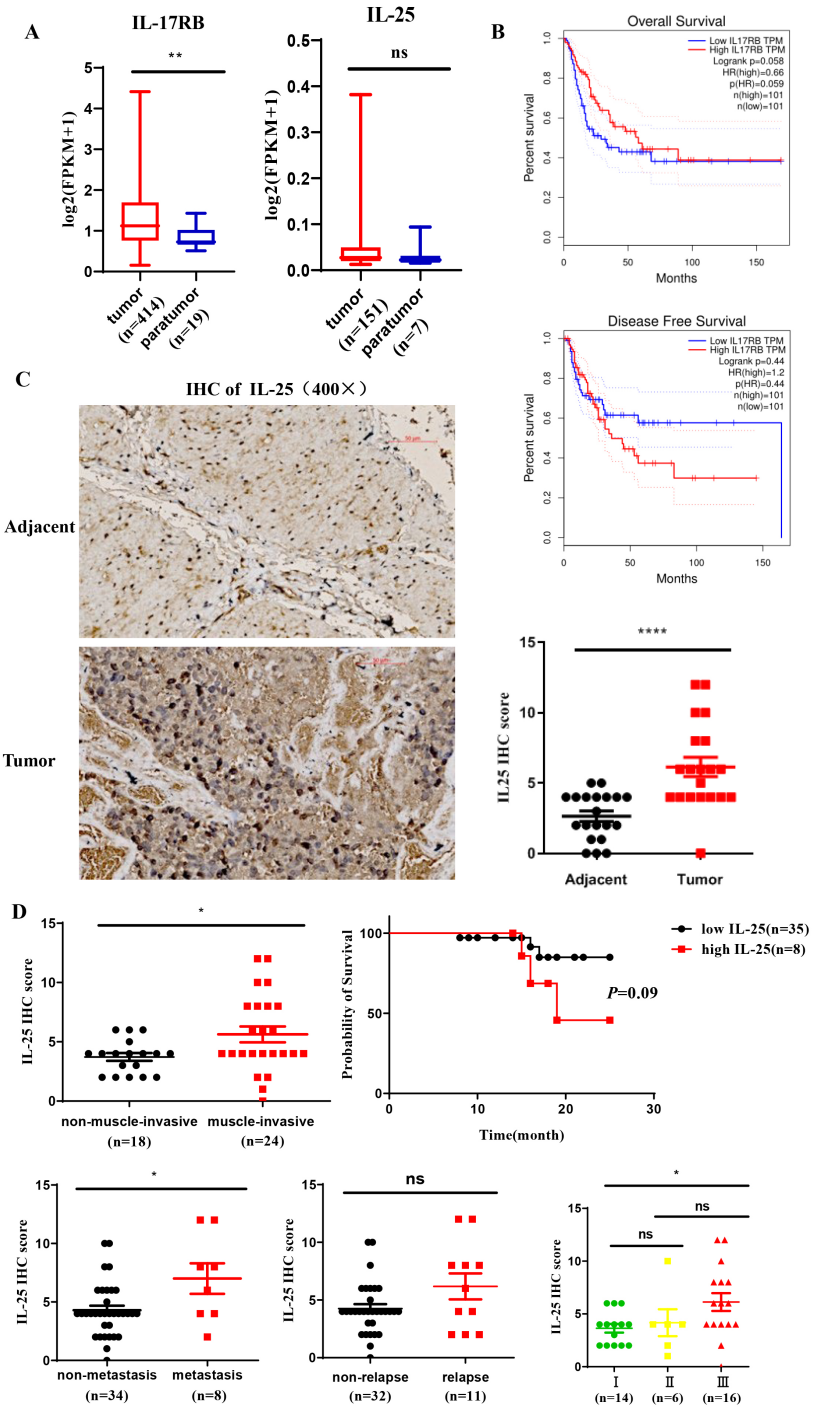

Fig. 1. Expression patterns of interleukin (IL)-25 and interleukin-17 receptor B (IL-17RB) in Bladder cancer (BCa) patients and their clinical correlation. (A) Expression levels of IL-17RB and IL-25 in BCa (left) and adjacent tissues (right) from The Cancer Genome Atlas (TCGA) database. (B) Overall survival (OS) and disease-free survival (DFS) in BCa patients based on IL-17RB expression levels using GEPIA2. Patients were grouped into high (red, 25%) and low (blue, 75%) IL-17RB expression groups. Log-rank *p*-value < 0.05 was considered statistically significant. (C) Representative images of IL-25 IHC staining in a clinical sample of human BCa and adjacent tissues (400× magnification). Scale bar: 50 μm. Immunohistochemical scoring was calculated by multiplying staining intensity by staining frequency. (D) Correlation of IL-25 expression with muscle invasion, survival, metastasis, recurrence, and different clinical stages of bladder cancer. High IL-25 expression was considered as an IHC-Score >6. Data are presented as the mean ± SEM, ns (no significance), * $p < 0.05$, ** $p < 0.01$, **** $p < 0.0001$. GEPIA2, gene expression profiling interactive analysis 2; SEM, standard error of mean; IHC, immunohistochemical.

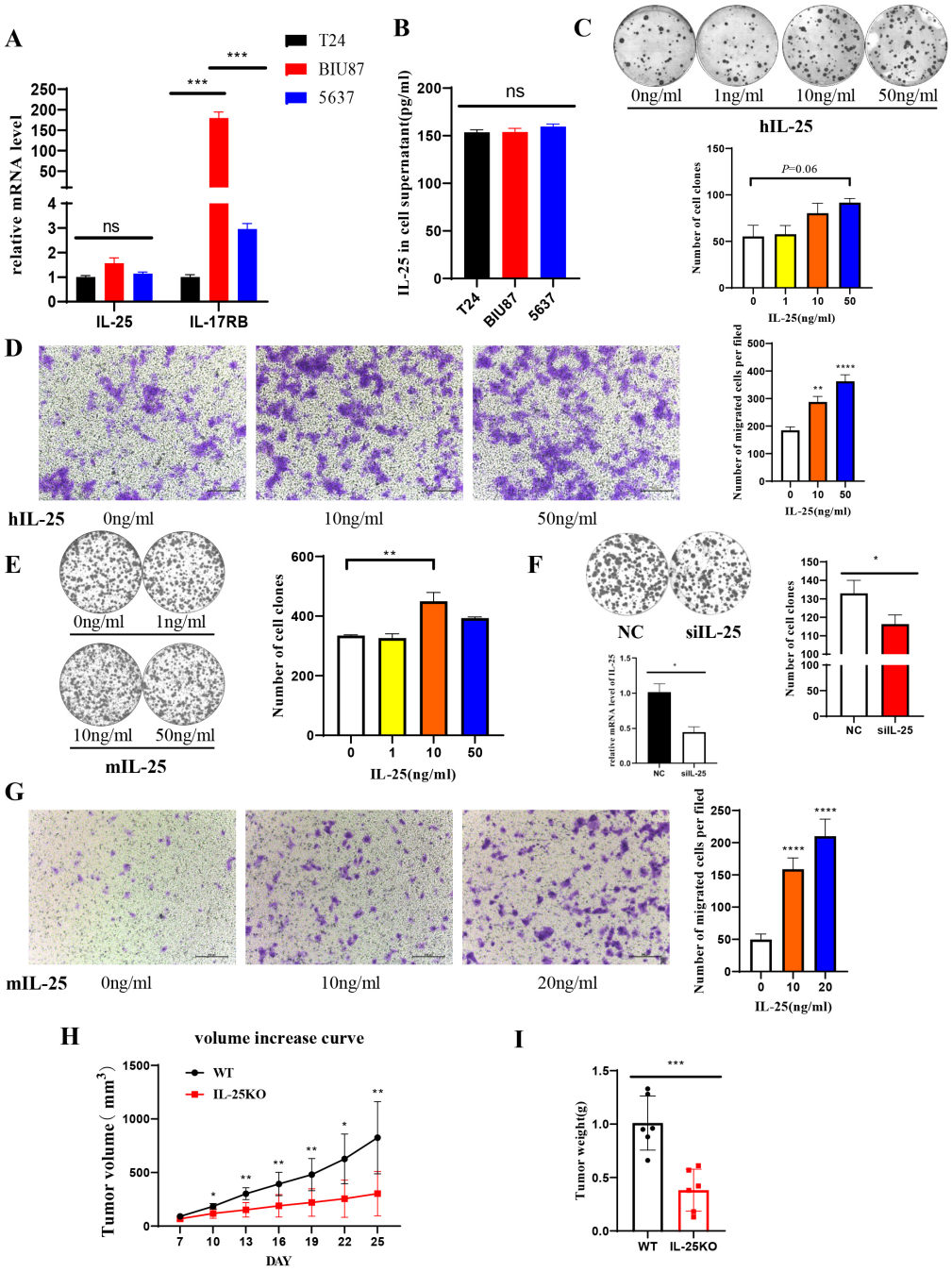

Fig. 2. Impacts of IL-25 on proliferation, migration of BCa cell lines, and subcutaneous tumor growth inhibition in IL-25 knockout mice. (A) mRNA expression levels of *IL-17RB* and *IL-25* in three human BCa cell lines: T24 (black), BIU87 (red), and 5637 (blue). (B) Concentration of IL-25 in the culture supernatant of T24, BIU87, and 5637 cell lines. (C) Plate clone formation analysis of BIU87 cells treated with recombinant human IL-25 (hIL-25) in a dose-dependent manner. Representative images (top) and statistical plots (bottom). (D) Transwell cell migration analysis of BIU87 cells. Representative images (left, 100× magnification) and statistical plots (right). Scale bar: 200 μm. (E) Plate clone formation analysis of MB49 cells treated with recombinant mouse IL-25 (mIL-25) in a dose-dependent manner. (F) Plate clone formation analysis of MB49 cells following IL-25 silencing. (G) Transwell cell migration analysis of MB49 cells treated with IL-25 in a concentration-dependent manner. Representative images (left, 100× magnification) and statistical plots (right). Counting criteria: In the colony formation assay, a size >0.035 inch^2 was considered a cell clone. In the transwell migration assay, a size >0.0003 mm^2 was considered a cell. Data are presented as the mean ± SEM, ordinary one-way analysis of variance (ANOVA) and Dunnett's multiple comparisons test. (H) Subcutaneous tumor volume growth curve of bladder cancer in wild-type (WT) (n = 6) and IL-25 knockout (IL-25KO) (n = 6) mice. (I) Tumor weight of WT and IL-25KO mice. Data are presented as the mean ± SD. * $p < 0.05$, ** $p < 0.01$, *** $p < 0.001$, **** $p < 0.0001$, ns, no significance. SD, standard deviation.

Journal of
BIOLOGICAL REGULATORS
and Homeostatic Agents

companied with reduced PCNA and Cyclin D1 expression. These changes correspond inversely to those observed upon IL-25 treatment. Collectively, these findings indicate that IL-25 may promote BCa proliferation through activation of the AKT/mTOR pathway.

Angiogenesis Inhibition in Bladder Cancer of IL-25KO Mice

Tumor angiogenesis is critical in tumor proliferation. Upon examination of tumor tissue from mice, we observed a notable difference in blood vessel abundance between WT and IL-25KO mice. Fluorescence quantitative PCR and immunohistochemical staining were performed to investigate angiogenic differences. Our results revealed the downregulation of vascular endothlial growth factor (*VEGFA*, *VEGFB*), and placental growth factor (*PGF*) in IL-25KO mice compared to WT mice (Fig. 4A). Immunohistochemical staining of CD31 further confirmed a significant decrease in microvessel density in BCa tissues of IL-25KO mice relative to WT mice (Fig. 4B). Collectively, these findings indicate a suppression of angiogenesis in BCa tissue of IL-25KO mice.

Discussion

This study confirmed that IL-25 contributes to the initiation and progression of bladder cancer. Through bioinformatic analyses and immunohistochemical assessments of human clinical samples, we observed that IL-25 and its receptor IL-17RB are overexpressed in bladder cancer tissues, consistent with their expression profiles across various cancers. Clinical follow-up revealed that aberrant expression of IL-25 is associated with key indicators of bladder cancer progression, such as stage, metastasis, muscle invasion, and recurrence. However, due to incomplete follow-up data, the relationship between IL-25, IL-17RB expression, and patient survival remains unclear. Survival analysis indicated that while the overall survival rate was slightly higher or unchanged, the disease -free survival rate was lower in patients with high IL-17RB expression at advanced stages (50 or 100 months). This observation suggests that high expression of IL-17RB might influence bladder cancer progression.

This study had limitations in testing clinical samples related to bladder cancer. Notably, normal bladder tissue samples were not examined, which could provide a baseline for comparison. Additionally, existing literature, such as the study by Liu *et al*. [25], suggests that IL-25 and IL-17RB expressions are higher in cystitis than in bladder cancer. We plan to include these tissue types in our subsequent research to further elucidate the role of IL-25 in bladder cancer pathogenesis.

In vitro experiments demonstrated that IL-25 treatment enhances proliferation and migration in bladder cancer cell lines, corroborating findings from previous cell studies. Animal model results further supported these findings, with IL-25KO mice exhibiting slower tumor growth and reduced tumor volumes. Collectively, these results strengthen the evidence for the role of IL-25 in promoting the onset and progression of bladder cancer, underscoring the need for continued investigation into its biological mechanisms and potential as a therapeutic target.

We initially explored the specific mechanisms underlying bladder cancer progression through bioinformatics analysis. GSEA enrichment analysis suggested that IL-17RB is likely associated with the NOD-like receptor signaling pathway. NOD-like receptors, primarily NOD1 and NOD2 [27], are known to activate the nuclear factor kappa-B (NF-κB), mitogen-activated protein kinase (MAPK) signaling pathways, and the inflammasome pathway [28], which includes NOD-like receptor thermal protein domain associated protein 3 (NLRP3). These pathways can lead to the activation of caspase-1, which in turn matures pro-inflammatory cytokines such as IL-1β and IL-18 (https://www.kegg.jp/entry/map04621). Previous research by Duan *et al*. [29] demonstrated that NOD2 induces IL-25 expression in the lung.

Our experimental data suggest that IL-25 promotes *NOD2* expression in bladder cancer. The NOD-like receptor signaling pathway is closely associated with inflammatory responses, and IL-25 and its receptor IL-17RB have also been reported to play an important role in inflammation. We hypothesized that IL-25 promotes bladder cancer progression by inducing inflammation through NOD-like receptor signaling. However, our investigation did not support this hypothesis for several reasons. Firstly, after IL-25 knockout or IL-25 treatment, we observed no significant changes in the expression levels of other key genes in this pathway, except *NOD2*, including the critical inflammatory molecule NF-κB. Secondly, bioinformatic analysis indicated upregulated *NOD2* expression in the low IL-17RB expression group, whereas experimental data showed increased *NOD2* expression following IL-25 treatment, suggesting inconsistent effects of IL-17RB and IL-25 on *NOD2* expression. Thirdly, RIP2 (phosphatidylinositol-4,5-bisphosphate), a serine-threonine and tyrosine kinase downstream of NOD1 and NOD2, plays a significant role in these pathways. RIP2KO mice have larger bladder cancer tumors and higher incidence and metastasis rates [30]. However, in our study, the expression of Ripk2 in the bladder cancer of IL-25KO mice was downregulated, but the tumor volume was smaller. Therefore, we gave up studying this signaling pathway in depth.

Numerous studies have demonstrated that the activation of the phosphatidylinositide 3-kinases (PI3K)/AKT/mTOR pathway is closely related to the onset and progression of cancer [31–33]. This pathway is critical in fundamental cellular processes such as metabolism, growth, proliferation, apoptosis, and angiogenesis. Ligands such as insulin or insulin-like growth

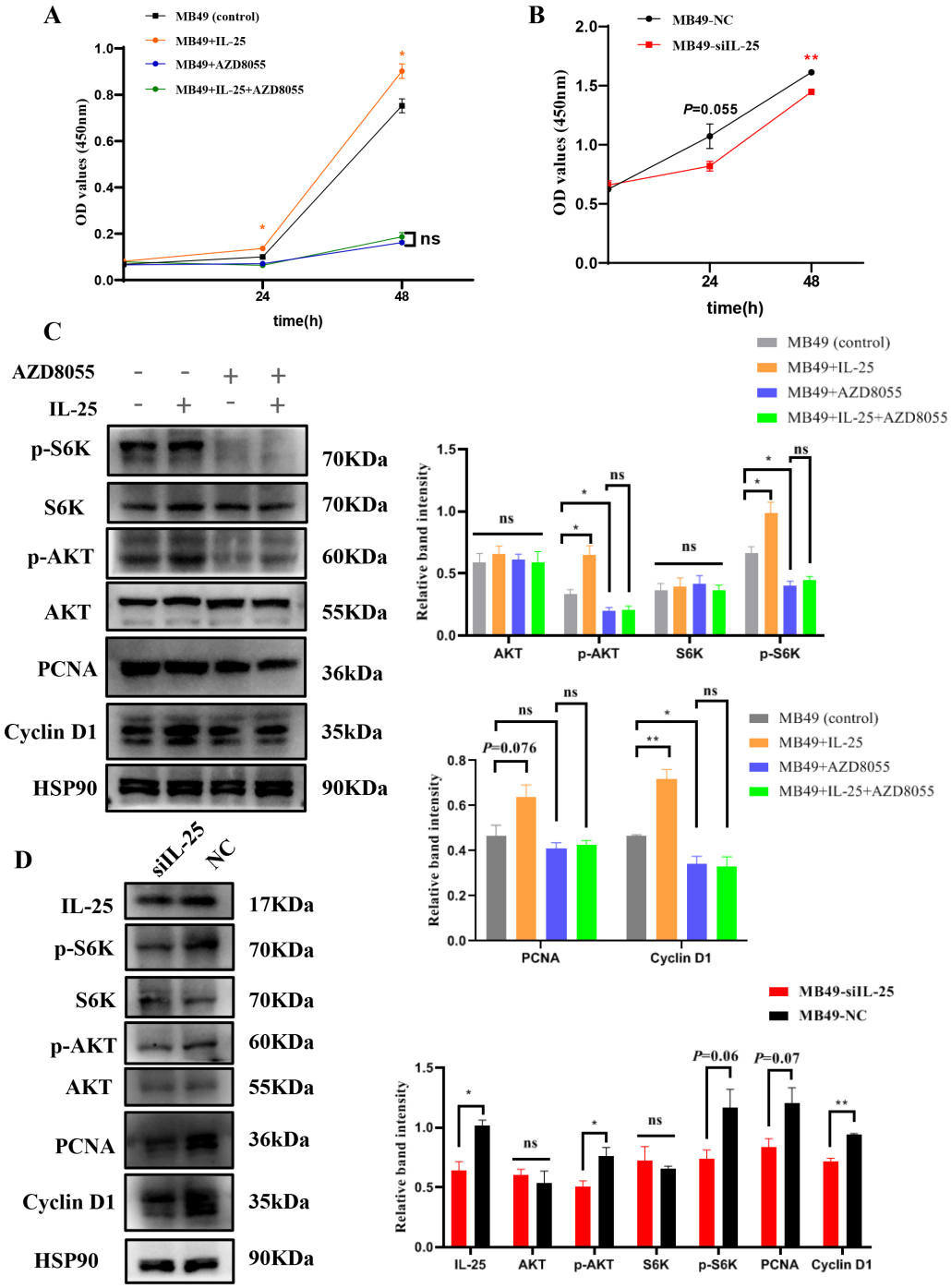

Fig. 3. IL-25 activates the AKT/mTOR signaling pathway to promote bladder cancer cell proliferation. (A) Cell viability of MB49 cells treated with IL-25 (50 ng/mL) or AZD8055 (0.5 μM) was measured using the Cell Counting Kit-8 (CCK-8) assay. *$p < 0.05$ versus the MB49 (control) group, ns versus the group treated with AZD8055 (0.5 μM). (B) CCK-8 assay detected the cell viability in MB49 after IL-25 knockdown. **$p < 0.01$ versus the MB49-NC group. Data are presented as the mean ± SEM. (Ordinary one-way analysis of variance (ANOVA) and Dunnett's multiple comparisons test). (C) Phosphorylation levels of S6K and AKT, and expression levels of PCNA and Cyclin D1 in MB49 cells after treatment with IL-25 (50 ng/mL) or AZD8055 (0.5 μM). The statistical graph is presented on the right. Data are presented as the mean ± SEM. (D) Phosphorylation levels of S6K and AKT, and expression levels of PCNA and Cyclin D1 in MB49 after knockdown of IL-25 by siRNA. The statistical graph is presented on the right. Data are presented as the mean ± SEM, ns (no significance), * $p < 0.05$, **$p < 0.01$. (Unpaired *t*-test). AKT, protein kinase B; mTOR, mammalian target of rapamycin; S6K, ribosomaiprotein S6 kinase; PCNA, proliferating cell nuclear antigen; HSP90, heat shock proteins 90.

Journal of
BIOLOGICAL REGULATORS
and Homeostatic Agents

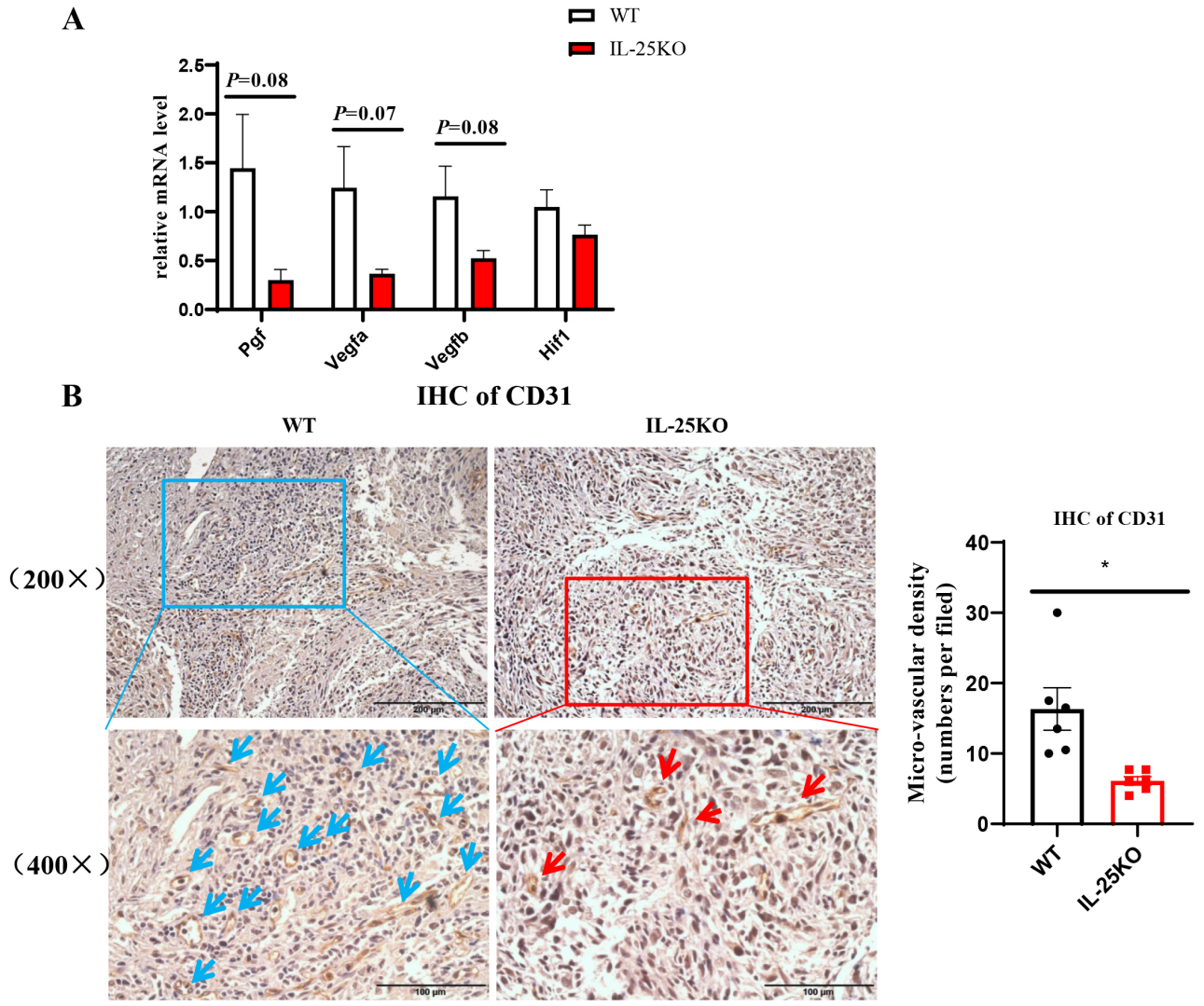

Fig. 4. Inhibition of angiogenesis in bladder cancer of IL-25 knockout mice. (A) mRNA expression levels of angiogenesis-related cytokines in bladder cancer tissues of WT and IL-25KO mice. (B) CD31 immunohistochemical staining and microvessel density statistics of bladder cancer tissues from WT and IL-25KO mice. The blue arrow points to the vascular position of WT mice, and the red arrow points to the vascular position of IL-25KO mice. Two to four fields of view were randomly selected for each section for imaging, and the number of microvessels was counted. The average value was used for statistical analysis. Data are presented as the mean ± SEM. *$p < 0.05$.

factors activate this pathway, involving receptor tyrosine kinases (RTKs) or G protein-coupled receptors (GPCRs). By reactivating downstream PI3K, AKT is fully activated through two phosphorylation processes, among which mTORC2 phosphorylates Ser473 of AKT [34]. Activated AKT ultimately leads to the activation of mTORC1 through phosphorylation of its downstream molecules [35,36]. mTORC1 further phosphorylates ribosomal protein S6 (rpS6) through S6K activation, enhancing protein translation [37,38]. The phosphorylation status of S6K is commonly used to assess mTORC1 activity [39,40].

AKT, having more than 100 downstream substrates [41], regulates the cell cycle by inhibiting glycogen synthase kinase 3 (GSK3) and preventing the degradation of β-catenin, thus inducing the expression of Cyclin D1 [42]. In this study, we investigated whether IL-25 influences bladder cancer progression through the AKT/mTOR signaling pathway. Our results indicated that IL-25 could activate mTOR and AKT pathways, promoting cell proliferation and enhancing the expression of proliferating cell nuclear antigen (PCNA) and Cyclin D1.

In tumor tissues, blood vessels provide oxygen and nutrition for tumor cells, and the rapid proliferation of tumor cells will form an anoxic microenvironment, which will stimulate the generation of hypoxia-inducing factors and induce angiogenesis [43,44]. The PI3K/AKT/mTOR signaling cascade activation upregulates the mRNA transcription and protein translation of Hypoxia-inducible factor 1α

(HIF-1α) [45]. Binding of HIF-1α to vascular endothelial growth factor (VEGF) enhances transcription and promotes angiogenesis [46]. Through a comprehensive literature review, we identified a strong association between IL-25 and angiogenesis in tumor tissues [47]. IL-25 has been reported to enhance VEGF/VEGFR expression in endothelial cells through PI3K/AKT and MAPK pathways, thereby promoting angiogenesis [48].

Consistent with previous findings, our study demonstrated that VEGF expression was downregulated in the IL-25KO group, and the number of microvessels in the IL-25KO mice was less than that in the WT group. In summary, our findings suggest that IL-25 promotes the progression of bladder cancer by activating the AKT/mTOR-regulated signaling pathway, leading to increased proliferation and enhanced angiogenesis. This study provides valuable evidence supporting IL-25 as a potential therapeutic target for bladder cancer management.

The treatment of bladder cancer adopts different treatment methods according to the degree of invasion. The primary treatment of NMIBC is transurethral resection of bladder tumor, supplemented with intravesical instillation of chemotherapy or immunotherapy agents to prevent recurrence and tumor progression [49,50]. Bacillus calmette-guerin (BCG) immunotherapy is a conservative approach to inhibit NMIBC progression [51]. In case of MIBC, patients typically undergo radical cystectomy and pelvic lymph node dissection, followed by combined neoadjuvant chemotherapy [52]. Aurelie Kamoun *et al.* [53] classified MIBC into six molecular subtypes: luminal papillary (24%), luminal non-specified (8%), luminal unstable (15%), stroma-rich (15%), basal/squamous (35%), and neuroendocrine-like (3%). The association between IL-25 and these molecular subtypes needs further investigation. In 2021, XKH001, the first monoclonal antibody targeting IL-25, developed by Dong Chen from the Chinese Academy of Sciences, received FDA approval for clinical trials in treating asthma (NCT05128409 and NCT05991661). Therefore, in addition to further determining the role of IL-25 in different molecular subtypes, we aim to use this drug to validate its therapeutic efficacy in bladder cancer. These efforts are anticipated to establish a foundation for using IL-25 as a biomarker to classify and diagnose bladder cancer, potentially enhancing targeted treatment strategies.

Conclusion

Our findings revealed that elevated expressions of IL-25 and its receptor IL-17RB are associated with accelerated progression of BCa. IL-25 can promote the proliferation and migration of human and mouse bladder cancer cells. IL-25 promoted cell proliferation by activating AKT/mTOR signaling pathway. IL-25 knockdown inhibits angiogenesis. This study elucidated the role and mechanism of IL-25 in promoting the progression of bladder cancer, and provided a new target and theoretical basis for the treatment of bladder cancer.

Availability of Data and Materials

The data used to support these findings of this study are available from the corresponding authors upon request.

Author Contributions

JS performed the experiments and wrote the first draft of the manuscript. JS and ZZ worked together on the collection of associated data and revised the manuscript. ZZ provided help and suggestions for the advancement of experiments and research. YH provided clinical samples for our research and made irreplaceable contributions to the acquisition of clinical experimental data. And in the improvement and promotion of the research, he put forward some constructive opinions and plans. ZY provided all the costs for the experiment in the study, and discussed the data. YH and ZY provided insightful discussions and useful suggestions for the study. All authors contributed to important editorial changes in the manuscript. All authors read and approved the final manuscript. All authors have participated sufficiently in the work and agreed to be accountable for all aspects of the work.

Ethics Approval and Consent to Participate

All patients provided informed consent, and the study protocol was approved by the Ethics Committee of the First Affiliated Hospital of Sun Yat-sen University (IRB no. [2019] 342). All mice were housed at the Laboratory Animal Center of Sun Yat-sen Medical College, and the experimental procedures were approved by the Institutional Animal Care and Use Committee (IACUC) of Sun Yat-sen University (Approval No. SYSU-IACUC-MED-2023-B082).

Acknowledgment

Not applicable.

Funding

This research was funded by the Fund of Shenzhen Key Laboratory (grant number: ZDSYS20220606100803007) received by ZY.

Conflict of Interest

The authors declare no conflict of interest.

Supplementary Material

Supplementary material associated with this article can be found, in the online version, at https://doi.org/10.23812/j.biol.regul.homeost.agents.20243807.451.

Journal of
BIOLOGICAL REGULATORS
and Homeostatic Agents

References

[1] Lenis AT, Lec PM, Chamie K, Mshs MD. Bladder Cancer: A Review. JAMA. 2020; 324: 1980–1991.

[2] Ahmadi H, Duddalwar V, Daneshmand S. Diagnosis and Staging of Bladder Cancer. Hematology/oncology Clinics of North America. 2021; 35: 531–541.

[3] Charlton ME, Adamo MP, Sun L, Deorah S. Bladder cancer collaborative stage variables and their data quality, usage, and clinical implications: a review of SEER data, 2004-2010. Cancer. 2014; 120: 3815–3825.

[4] Dobruch J, Oszczudłowski M. Bladder Cancer: Current Challenges and Future Directions. Medicina (Kaunas, Lithuania). 2021; 57: 749.

[5] Teoh JYC, Kamat AM, Black PC, Grivas P, Shariat SF, Babjuk M. Recurrence mechanisms of non-muscle-invasive bladder cancer - a clinical perspective. Nature Reviews. Urology. 2022; 19: 280–294.

[6] Amling CL. Diagnosis and management of superficial bladder cancer. Current Problems in Cancer. 2001; 25: 219–278.

[7] Bray F, Ferlay J, Soerjomataram I, Siegel RL, Torre LA, Jemal A. Global cancer statistics 2018: GLOBOCAN estimates of incidence and mortality worldwide for 36 cancers in 185 countries. CA: a Cancer Journal for Clinicians. 2018; 68: 394–424.

[8] Deng C, Peng N, Tang Y, Yu N, Wang C, Cai X, *et al*. Roles of IL-25 in Type 2 Inflammation and Autoimmune Pathogenesis. Frontiers in Immunology. 2021; 12: 691559.

[9] Fort MM, Cheung J, Yen D, Li J, Zurawski SM, Lo S, *et al*. IL-25 induces IL-4, IL-5, and IL-13 and Th2-associated pathologies in vivo. Immunity. 2001; 15: 985–995.

[10] Su J, Chen T, Ji XY, Liu C, Yadav PK, Wu R, *et al*. IL-25 downregulates Th1/Th17 immune response in an IL-10-dependent manner in inflammatory bowel disease. Inflammatory Bowel Diseases. 2013; 19: 720–728.

[11] Emamaullee JA, Davis J, Merani S, Toso C, Elliott JF, Thiesen A, *et al*. Inhibition of Th17 cells regulates autoimmune diabetes in NOD mice. Diabetes. 2009; 58: 1302–1311.

[12] Min HK, Won JY, Kim BM, Lee KA, Lee SJ, Lee SH, *et al*. Interleukin (IL)-25 suppresses IL-22-induced osteoclastogenesis in rheumatoid arthritis via STAT3 and p38 MAPK/IκBα pathway. Arthritis Research & Therapy. 2020; 22: 222.

[13] Kleinschek MA, Owyang AM, Joyce-Shaikh B, Langrish CL, Chen Y, Gorman DM, *et al*. IL-25 regulates Th17 function in autoimmune inflammation. The Journal of Experimental Medicine. 2007; 204: 161–170.

[14] Xu M, Lu H, Lee YH, Wu Y, Liu K, Shi Y, *et al*. An Interleukin-25-Mediated Autoregulatory Circuit in Keratinocytes Plays a Pivotal Role in Psoriatic Skin Inflammation. Immunity. 2018; 48: 787–798.e4.

[15] Borowczyk J, Buerger C, Tadjrischi N, Drukala J, Wolnicki M, Wnuk D, *et al*. IL-17E (IL-25) and IL-17A Differentially Affect the Functions of Human Keratinocytes. The Journal of Investigative Dermatology. 2020; 140: 1379–1389.e2.

[16] Huang CK, Yang CY, Jeng YM, Chen CL, Wu HH, Chang YC, *et al*. Autocrine/paracrine mechanism of interleukin-17B receptor promotes breast tumorigenesis through NF-κB-mediated antiapoptotic pathway. Oncogene. 2014; 33: 2968–2977.

[17] Borowczyk J, Shutova M, Brembilla NC, Boehncke WH. IL-25 (IL-17E) in epithelial immunology and pathophysiology. The Journal of Allergy and Clinical Immunology. 2021; 148: 40–52.

[18] Lee JB, Chen CY, Liu B, Mugge L, Angkasekwinai P, Facchinetti V, *et al*. IL-25 and CD4(+) TH2 cells enhance type 2 innate lymphoid cell-derived IL-13 production, which promotes IgE-mediated experimental food allergy. The Journal of Allergy and Clinical Immunology. 2016; 137: 1216–1225.e5.

[19] Kaewsarabhumi S, Proungvitaya T, Limpaiboon T, Tippayawat P, Tummanatsakun D, Titapun A, *et al*. Interleukin 25 (IL-25) expression in cholangiocarcinoma. Molecular and Clinical Oncology. 2020; 13: 84.

[20] Guo F, Ru Q, Zhang J, He S, Yu J, Zheng S, *et al*. Inflammation factors in hepatoblastoma and their clinical significance as diagnostic and prognostic biomarkers. Journal of Pediatric Surgery. 2017; 52: 1496–1502.

[21] Wei C, Sirikanjanapong S, Lieberman S, Delacure M, Martiniuk F, Levis W, *et al*. Primary mucosal melanoma arising from the eustachian tube with CTLA-4, IL-17A, IL-17C, and IL-17E upregulation. Ear, Nose, & Throat Journal. 2013; 92: 36–40.

[22] Li Q, Ma L, Shen S, Guo Y, Cao Q, Cai X, *et al*. Intestinal dysbacteriosis-induced IL-25 promotes development of HCC via alternative activation of macrophages in tumor microenvironment. Journal of Experimental & Clinical Cancer Research: CR. 2019; 38: 303.

[23] Liu J, Qian B, Zhou L, Shen G, Tan Y, Liu S, *et al*. IL25 Enhanced Colitis-Associated Tumorigenesis in Mice by Upregulating Transcription Factor GLI1. Frontiers in Immunology. 2022; 13: 837262.

[24] Benatar T, Cao MY, Lee Y, Lightfoot J, Feng N, Gu X, *et al*. IL-17E, a proinflammatory cytokine, has antitumor efficacy against several tumor types in vivo. Cancer Immunology, Immunotherapy: CII. 2010; 59: 805–817.

[25] Liu Y, Yang W, Zhao L, Liang Z, Shen W, Hou Q, *et al*. Immune analysis of expression of IL-17 relative ligands and their receptors in bladder cancer: comparison with polyp and cystitis. BMC Immunology. 2016; 17: 36.

[26] Yin H, Gao T, Xie J, Huang Z, Zhang X, Yang F, *et al*. FUBP1 promotes colorectal cancer stemness and metastasis via DVL1-mediated activation of Wnt/β-catenin signaling. Molecular Oncology. 2021; 15: 3490–3512.

[27] Li D, Wu M. Pattern recognition receptors in health and diseases. Signal Transduction and Targeted Therapy. 2021; 6: 291.

[28] Poli G, Fabi C, Bellet MM, Costantini C, Nunziangeli L, Romani L, *et al*. Epigenetic Mechanisms of Inflammasome Regulation. International Journal of Molecular Sciences. 2020; 21: 5758.

[29] Duan W, Mehta AK, Magalhaes JG, Ziegler SF, Dong C, Philpott DJ, *et al*. Innate signals from Nod2 block respiratory tolerance and program T(H)2-driven allergic inflammation. The Journal of Allergy and Clinical Immunology. 2010; 126: 1284–93.e10.

[30] Zhang H, Chin AI. Role of Rip2 in development of tumor-infiltrating MDSCs and bladder cancer metastasis. PloS One. 2014; 9: e94793.

[31] Duan Y, Haybaeck J, Yang Z. Therapeutic Potential of PI3K/AKT/mTOR Pathway in Gastrointestinal Stromal Tumors: Rationale and Progress. Cancers. 2020; 12: 2972.

[32] Sun EJ, Wankell M, Palamuthusingam P, McFarlane C, Hebbard L. Targeting the PI3K/Akt/mTOR Pathway in Hepatocellular Carcinoma. Biomedicines. 2021; 9: 1639.

[33] Miricescu D, Totan A, Stanescu-Spinu II, Badoiu SC, Stefani C, Greabu M. PI3K/AKT/mTOR Signaling Pathway in Breast Cancer: From Molecular Landscape to Clinical Aspects. International Journal of Molecular Sciences. 2020; 22: 173.

[34] Kakumoto K, Ikeda JI, Okada M, Morii E, Oneyama C. mLST8 Promotes mTOR-Mediated Tumor Progression. PloS One. 2015; 10: e0119015.

[35] Berchtold D, Walther TC. TORC2 plasma membrane localization is essential for cell viability and restricted to a distinct domain. Molecular Biology of the Cell. 2009; 20: 1565–1575.

[36] Um SH, D'Alessio D, Thomas G. Nutrient overload, insulin resistance, and ribosomal protein S6 kinase 1, S6K1. Cell Metabolism. 2006; 3: 393–402.

[37] Faivre S, Kroemer G, Raymond E. Current development of mTOR inhibitors as anticancer agents. Nature Reviews. Drug Discovery. 2006; 5: 671–688.

[38] Osaki M, Oshimura M, Ito H. PI3K-Akt pathway: its functions and alterations in human cancer. Apoptosis: an International Journal on Programmed Cell Death. 2004; 9: 667–676.

[39] Lim HK, Choi YA, Park W, Lee T, Ryu SH, Kim SY, *et al*. Phosphatidic acid regulates systemic inflammatory responses by modulating the Akt-mammalian target of rapamycin-p70 S6 kinase 1 pathway. The Journal of Biological Chemistry. 2003; 278: 45117–45127.

[40] Nojima H, Tokunaga C, Eguchi S, Oshiro N, Hidayat S, Yoshino KI, *et al*. The mammalian target of rapamycin (mTOR) partner, raptor, binds the mTOR substrates p70 S6 kinase and 4E-BP1 through their TOR signaling (TOS) motif. The Journal of Biological Chemistry. 2003; 278: 15461–15464.

[41] Manning BD, Toker A. AKT/PKB Signaling: Navigating the Network. Cell. 2017; 169: 381–405.

[42] Diehl JA, Cheng M, Roussel MF, Sherr CJ. Glycogen synthase kinase-3beta regulates cyclin D1 proteolysis and subcellular localization. Genes & Development. 1998; 12: 3499–3511.

[43] Courtnay R, Ngo DC, Malik N, Ververis K, Tortorella SM, Karagiannis TC. Cancer metabolism and the Warburg effect: the role of HIF-1 and PI3K. Molecular Biology Reports. 2015; 42: 841–851.

[44] Risau W. Mechanisms of angiogenesis. Nature. 1997; 386: 671–674.

[45] Semenza GL. HIF-1 mediates metabolic responses to intratumoral hypoxia and oncogenic mutations. The Journal of Clinical Investigation. 2013; 123: 3664–3671.

[46] Yee Koh M, Spivak-Kroizman TR, Powis G. HIF-1 regulation: not so easy come, easy go. Trends in Biochemical Sciences. 2008; 33: 526–534.

[47] Zhang F, Liu Y, Wang S, Yan X, Lin Y, Chen D, *et al*. Interleukin-25-Mediated-IL-17RB Upregulation Promotes Cutaneous Wound Healing in Diabetic Mice by Improving Endothelial Cell Functions. Frontiers in Immunology. 2022; 13: 809755.

[48] Corrigan CJ, Wang W, Meng Q, Fang C, Wu H, Reay V, *et al*. T-helper cell type 2 (Th2) memory T cell-potentiating cytokine IL-25 has the potential to promote angiogenesis in asthma. Proceedings of the National Academy of Sciences of the United States of America. 2011; 108: 1579–1584.

[49] Slovacek H, Zhuo J, Taylor JM. Approaches to Non-Muscle-Invasive Bladder Cancer. Current Oncology Reports. 2021; 23: 105.

[50] Babjuk M, Burger M, Compérat EM, Gontero P, Mostafid AH, Palou J, *et al*. European Association of Urology Guidelines on Non-muscle-invasive Bladder Cancer (TaT1 and Carcinoma In Situ) - 2019 Update. European Urology. 2019; 76: 639–657.

[51] Balar AV, Kamat AM, Kulkarni GS, Uchio EM, Boormans JL, Roumiguié M, *et al*. Pembrolizumab monotherapy for the treatment of high-risk non-muscle-invasive bladder cancer unresponsive to BCG (KEYNOTE-057): an open-label, single-arm, multicentre, phase 2 study. The Lancet. Oncology. 2021; 22: 919–930.

[52] Ma J, Black PC. Current Perioperative Therapy for Muscle Invasive Bladder Cancer. Hematology/oncology Clinics of North America. 2021; 35: 495–511.

[53] Kamoun A, de Reyniès A, Allory Y, Sjödahl G, Robertson AG, Seiler R, *et al*. A Consensus Molecular Classification of Muscle-invasive Bladder Cancer. European Urology. 2020; 77: 420–433.